Ocean Dynamics (2015) 65:419–434
DOI 10.1007/s10236-014-0807-5

East Frisian Wadden Sea hydrodynamics and wave effects in an unstructured-grid model

Sebastian Grashorn · Karsten A. Lettmann · Jörg-Olaf Wolff · Thomas H. Badewien · Emil V. Stanev

Received: 21 March 2013 / Accepted: 30 December 2014 / Published online: 3 February 2015

Abstract An unstructured-grid model (FVCOM) coupled to a surface wave model (FVCOM-SWAVE) with two different setups is used to investigate the hydrodynamic and wave energy conditions during a moderate wind and a storm situation in the southern North Sea. One setup covers the whole North Sea with moderately increased grid resolution at the coast, whereas the other is a very high-resolution Wadden Sea setup that is one-way coupled to the coarser North Sea model. The results of both model setups are validated, compared to each other and analysed with a focus on longshore currents and wave energy. The numerical results show that during storm conditions, strong wave-induced longshore currents occur in front of the East Frisian Wadden Sea islands with current speeds up to 1 m/s. The model setup with the higher resolution around the islands shows even stronger currents than the coarser setup. The wave-current interaction also influences the surface elevation by raising the water level in the tidal basins. The calculated wave energies show large differences between moderate wind and storm conditions with time-averaged values up to 200 kW/m.

Keywords Numerical modelling · FVCOM · Wave-current interaction · Longshore currents · Wave energy · Wadden Sea

1 Introduction

The German coast, located in the area of the southern part of the North Sea, has been exposed to storm surges and resultant floodings for hundreds of years. Hence, people living close to the coast tried to adapt themselves and their environment to prevent damage caused by extreme storm conditions and extreme sea levels. The latter can be caused by high astronomical tides, storm surges, locally wind-generated gravity waves (wind sea), swell or a changing sea level (see Weisse et al. 2012).

The barrier island system of the Dutch and German Wadden Sea and its various tidal inlets have been subject to many studies focusing on different features of this unique coastal system. Dastgheib et al. (2008), Dissanayake et al. (2009), Van der Wegen et al. (2010) and Yu et al. (2012) used models to investigate aspects of the long-term morphological evolution of tidal inlet areas. In the East Frisian Wadden Sea, Stanev et al. (2003a, b, 2007b, 2008) and Staneva et al. (2009) used numerical modelling tools and observational data to describe different physical aspects of the hydrodynamics in this area. Stanev et al. (2006, 2007a) investigated driving factors of sediment dynamics,

Responsible Editor: Martin Verlaan

This article is part of the Topical Collection on the *16th biennial workshop of the Joint Numerical Sea Modelling Group (JONSMOD) in Brest, France 21–23 May 2012*

S. Grashorn (✉) · E. V. Stanev
Helmholtz-Zentrum Geesthacht Centre for Materials and Coastal Research (HZG), Institute of Coastal Research, Max-Planck-Str. 1, 21502 Geesthacht, Germany
e-mail: sebastian.grashorn@hzg.de

K. A. Lettmann · J.-O. Wolff
Institute for Chemistry and Biology of the Marine Environment (ICBM), Department of Physical Oceanography (Theory), Carl von Ossietzky Universität Oldenburg, Carl-von-Ossietzky-Str. 9-11, 26111 Oldenburg, Germany

T. H. Badewien
Institute for Chemistry and Biology of the Marine Environment (ICBM), Department of Marine Sensor Systems, Carl von Ossietzky Universität Oldenburg, Carl-von-Ossietzky-Str. 9-11, 26111 Oldenburg, Germany

and Lettmann et al. (2009) focused on the response of sediment dynamics for different scenarios including storm conditions using numerical modelling. Reuter et al. (2009) and Bartholomä et al. (2009) used observational results to investigate similar aspects. Most of these papers conclude that the East Frisian Wadden Sea inlets are ebb-dominated.

This paper focuses on the impact of wave energy generated by wind on the currents in the area of the East Frisian Wadden Sea. A similar study for the area around the North Frisian Wadden Sea island of Sylt was conducted by Pleskachevsky et al. (2009).

Spectral wave models like WAM (WAMDI group 1988), TOMAWAC (Benoit 1996), SWAN (Booij et al. 1999) and WW3 (Tolman 2009) have matured over the last 20 years to a state capable of predicting the relevant wave parameters with a high degree of accuracy and are widely used even in coastal areas. Recently, the spectral wind wave model SWAN has been improved during a 5-year research program and the resulting statistical error parameters are considered small enough to determine reliable normative wave conditions in the Dutch Wadden Sea (see Van der Westhuysen et al. 2012). The coupling to ocean circulation models resulted in an ongoing effort on new theoretical approaches, numerical techniques and parameterizations (Roland and Ardhuin 2014). Gravity waves not only propagate on the surface of the ocean, they also have a profound effect on the currents in the ocean itself, especially in coastal areas.

The presence of surface waves in the shallow coastal ocean introduces an additional flux of momentum, the radiation stress (Longuet-Higgins and Stewart 1962, 1964), and its gradients can lead to changes in the mean water level known as wave setup or wave set-down. These wave-induced forces also lead to cross- and longshore currents, the latter being especially pronounced when waves approach the coast at a moderate angle.

The effects of wave-current interactions caused by radiation stresses (in a vertically averaged sense) have been subject to various studies (see, e.g. Longuet-Higgins 1970; Thornton and Guza 1986; Osuna and Monbaliu 2004; Pleskachevsky et al. 2009). Longuet-Higgins (1970) and Thornton and Guza (1986) derived equations for the magnitude of the wave-induced longshore current. Pleskachevsky et al. (2009) investigated the impact of a storm surge on the North Frisian island of Sylt by estimating the wave energy flux and the effects of wave-current interactions. Using a two-way-coupled modelling system, they found wave-induced currents of up to 1 m/s and maximum wave energy fluxes of about 160 kW/m in their area of interest. Osuna and Monbaliu (2004) investigated various aspects of wave-current interactions with a focus on the Belgian coast while Bolanos et al. (2008) and Brown et al. (2011, 2013) used a coupled modelling system based on the radiation stress formulation to evaluate the interaction effects in the area of the NW Mediterranean.

As wave effects are introduced into the system at the ocean surface, it is obvious that there is a vertical profile attached to the radiation stresses which will, amongst others, be important for sediment dynamics. Earlier studies of the three-dimensional distribution of the radiation stresses are based on a series of theoretical papers by Mellor (2003, 2005, 2008), which were derived correctly for flat bottom situations and therefore give consistent (vertically integrated) results to the theory of Longuet-Higgins and Stewart (Aiki and Greatbatch 2013). The applicability of Mellor's set of equations in situations with sloping bottom has been questioned by Ardhuin et al. (2008a, b) and Bennis and Ardhuin (2011) who suggested to use wave-averaged momentum equations derived from the three-dimensional Lagrangian mean framework of Andrews and McIntyre (1978) which include the so-called vortex force.

The effects of the two different approaches utilising the vortex force (see Ardhuin et al. 2008b) and the radiation stress (see Mellor 2008, 2011a, b) are compared by Moghimi et al. (2013). The implementations of both approaches were validated using flume experiments. By evaluating a realistic beach scenario, they found that the radiation stress formulation showed unrealistic offshore-directed transport in the wave-shoaling regions and close to steep bathymetry. On the other hand, the results for the longshore-directed transport are similar for both formulations. Brown et al. (2011) also questioned the reliability of the methods presented by Mellor (2003, 2008). Here, the authors connect inconsistencies to calculate the vertical flux within these methods to inaccuracies in the timing of the surge prediction.

In a recent series of papers, Aiki and Greatbatch (2012, 2013, 2014) have related the two seemingly different theories using a thickness-weighted-mean approach in a vertical Lagrangian and horizontal Eulerian sense. To the authors' knowledge, this new set of equations has not yet been used in coastal ocean numerical models. Because Aiki and Greatbatch (2013) stated that the radiation stress formulation of Mellor (2008) is applicable for small bottom slopes and Moghimi et al. (2013) found similar results of both methods at least for longshore currents, we concentrate in this paper on a discussion of the longshore currents.

An application of an unstructured-grid model that is two-way-coupled to a surface wave model with a high resolution of up to 50 m along the East Frisian barrier island chain to investigate the wave-induced longshore currents, and the energy flux along the coast has not been the focus of a study yet. In this contribution, the three-dimensional, unstructured grid modelling system FVCOM (see Chen et al. 2003; Qi et al. 2009), which is a 'combination' of the hydrodynamic model FVCOM and the wave model FVCOM-SWAVE, is used. This modelling system is applied to the North Sea and the East Frisian barrier island coast using two setups (one covering the whole North Sea and one covering only the East Frisian Wadden Sea) with a higher resolution in regions of interest and with a reduced resolution towards the open North Sea. FVCOM utilises the radiation stress formulation to describe the coupling procedure between the hydrodynamic model and the wave model. The Wadden Sea setup with the high resolution of up to 50 m is one-way coupled to the coarser North Sea model. For an overview of other approaches to unstructured grid modelling, we refer to Timmermann et al. (2009).

The study presented in this contribution aims to (i) test and discuss the usage and reliability of an unstructured-grid ocean model in the North Sea and the East Frisian Wadden Sea; (ii) compare the results given by a coarse North Sea model and a highly resolved Wadden Sea model; and (iii) discuss the effects of the wave-current interaction and the wave energy input at the East Frisian Wadden Sea coast for moderate wind and storm conditions.

2 Study site

The study site is located in the southern part of the North Sea and includes the west-east oriented barrier island chain along the northwestern coast of Germany (see Figs. 1 and 2). The area is characterized by several tidal basins, tidal flats and tidal inlets connected to the open North Sea. A tidal amplitude of 1.5 m is reached during spring tides and of 1.0 m during neap tides (see Lettmann et al. 2009) and thus the area can be identified as a mesotidal zone (see Flemming and Bartholomä 1997; Stanev et al. 2003b). The current velocity can reach a maximum of 1.5 m/s in the channels (see Santamarina Cuneo and Flemming 2000) and 0.35 m/s on the tidal flats (see Flemming and Delafontaine 1994). Krögel and Flemming (1998) summarise that the energy flux in the tidal catchment is controlled by the tidal currents, waves generated in the tidal basins and swells entering the inlet from the open North Sea. Most of the energy transported by the swells is dissipated over the ebb deltas and only about 10 % of the energy penetrates the inlets.

The southern North Sea region is located in an intermediate zone between the Iceland low-pressure and the Azores high-pressure system and was dominated in 2005 by

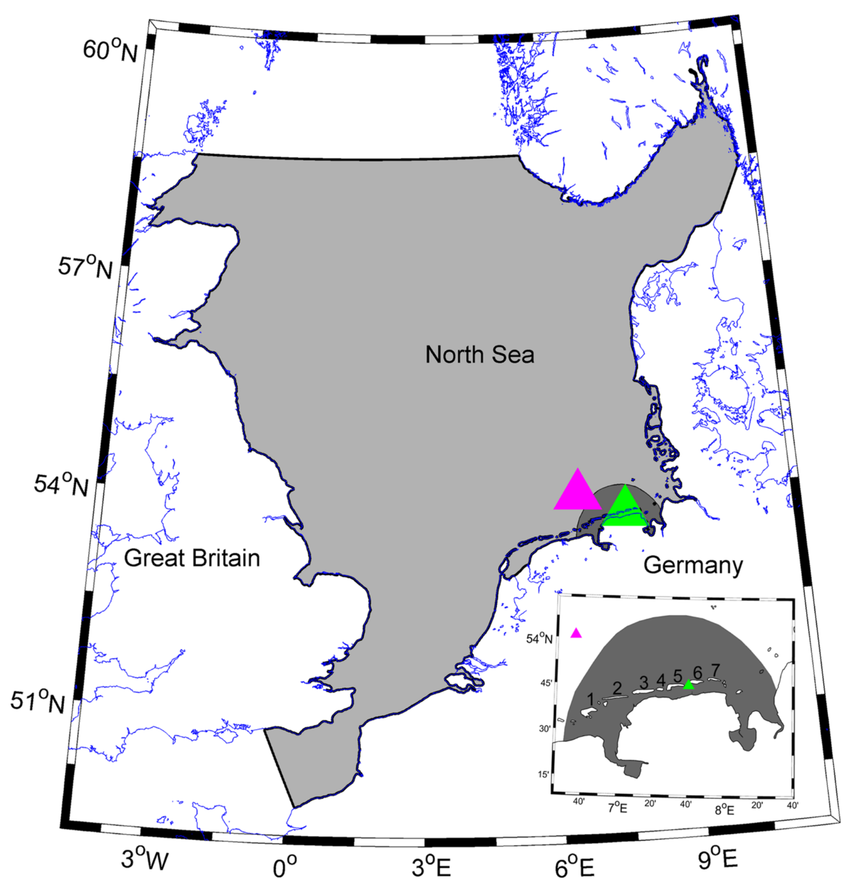

Fig. 1 Area of interest including the North Sea and the German Bight. The two *gray shaded areas* depict the coverage of the North Sea and the high-resolution Wadden Sea model. The Wadden Sea model is one-way coupled to the North Sea model. A zoom into the area of the East Frisian Wadden Sea can be seen in the lower right corner. The *magenta-coloured triangle* shows the position of the FINO I pile station and the *green triangle* the position of the ICBM pile station. The *numbers* indicate the main islands of the East Frisian Wadden Sea: 1 Borkum, 2 Juist, 3 Norderney, 4 Baltrum, 5 Langeoog, 6 Spiekeroog, 7 Wangerooge

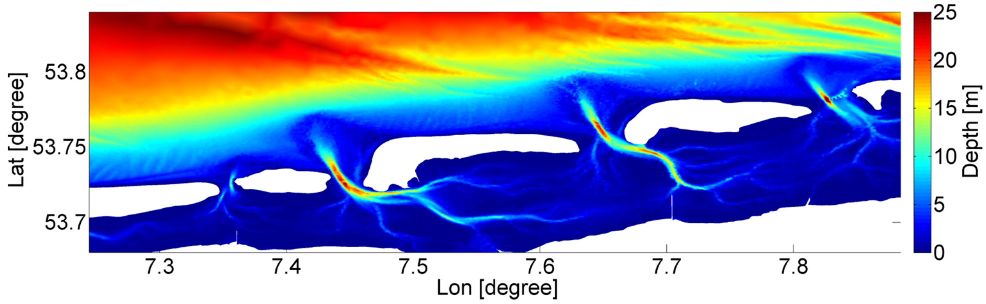

Fig. 2 Bathymetry of a part of the East Frisian Wadden Sea in the area of the islands Langeoog and Spiekeroog incorporating several tidal flats and basins (see also Fig. 1)

westerly winds (occurrence about 72 %) blowing from NW and W, in each case accounting for 36 % over the year (see Loewe 2009).

Figure 3 shows the joint distribution of the significant wave height and the peak period at the FINO I pile station (see Fig. 1) located close to the East Frisian Wadden Sea (data provided by the BSH, Federal Maritime and Hydrographic Agency of Germany). The figure displays the presence of wind-sea and swell-dominated sea states, with a dominant significant wave height of about 1.7 m and an associated peak period of about 6 s at the FINO I pile station. The joint distribution of the significant wave height and the wave direction (not shown) results in dominant waves propagating from the W-NW, with wave heights around 0.5 m.

At the pile station, operated by the Institute for Chemistry and Biology of the Marine Environment (ICBM) at the University of Oldenburg (see Figs. 1 and 4), the mean significant wave height was only about 0.36 m during Dec. 2006 until June 2007. This confirms that the wave energy reaching the mainland coast is substantially reduced along the barrier island chain (see also Lettmann et al. 2009).

3 Model

3.1 Model description

The computations were performed with the modelling system FVCOM, version 3.1.4. The Fortran-based FVCOM is a prognostic, unstructured-grid, finite-volume, free-surface, 3D primitive equations ocean model that was originally developed by Chen et al. (2003). The model solves the integral form of the governing equations for momentum, continuity, temperature, salinity and density by calculating the fluxes over a triangular mesh composed of non-overlapping horizontal control volumes using spherical coordinates (see manual provided by Chen et al. 2006). This can be done either in a 2D-mode with vertically integrated equations or in a 3D-mode. Tracers such as temperature, salinity or

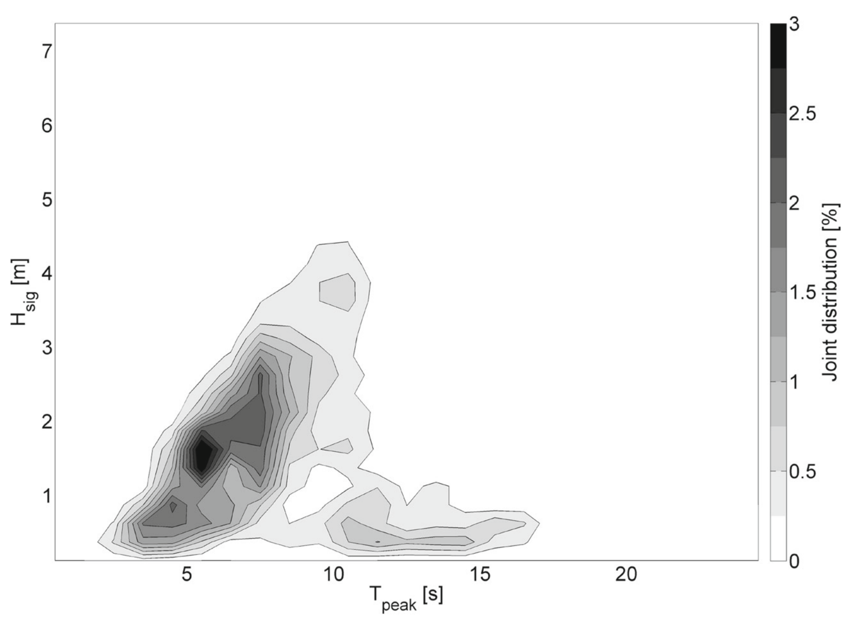

Fig. 3 Joint distribution of significant wave heights and peak periods at the FINO I wave buoy. The data was observed between December 2007 and June 2008

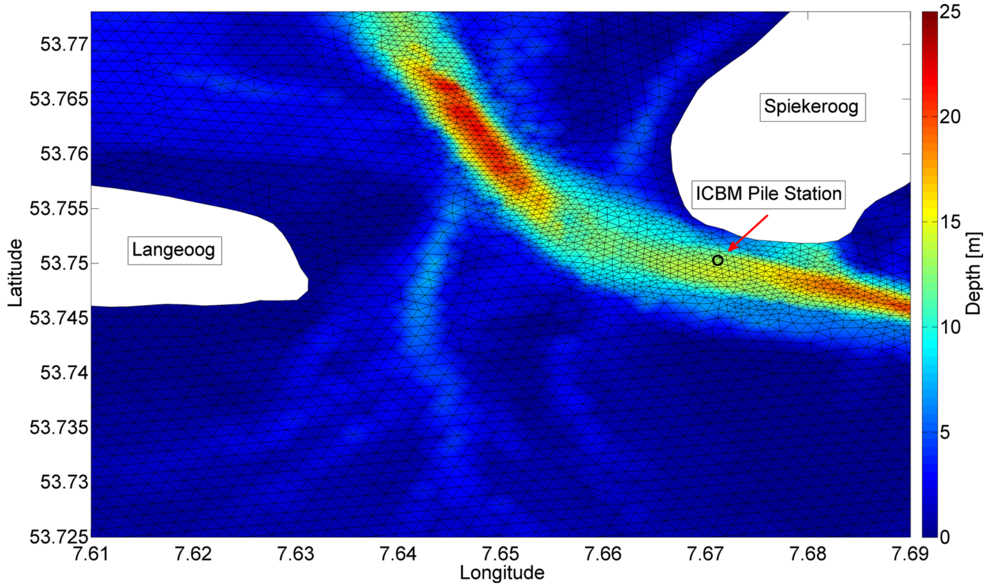

Fig. 4 Tidal channel between the barrier islands Langeoog and Spiekeroog. Here, the resolution of the mesh is increased to 50 m

surface elevation are calculated on each node of the unstructured triangles, while the velocities are calculated at the center of a triangle by the net flux through the three sides of that triangle.

The governing equations used by FVCOM are summarised by Wu et al. (2011) and were derived by Mellor (2003, 2005, 2008). The modified Mellor and Yamada level 2.5 (MY-2.5) and Smagorinsky turbulent closure schemes are used as default setups for vertical and horizontal mixing, respectively (see Mellor and Yamada 1982; Smagorinsky 1963; Wu et al. 2011). S_{xx}, S_{yy}, S_{xy} and S_{yx} are the radiation stress terms that describe the wave-current interaction and are defined by Mellor (2008) as

$$S_{xx} = kE\left(\frac{k_x^2}{k^2}F_{CS}F_{CC} - F_{SC}F_{SS}\right) + E_D \tag{1}$$

$$S_{yy} = kE\left(\frac{k_y^2}{k^2}F_{CS}F_{CC} - F_{SC}F_{SS}\right) + E_D \tag{2}$$

$$S_{xy} = S_{yx} = kE\frac{k_x k_y}{k^2}F_{CS}F_{CC} \tag{3}$$

with the wave energy E (see Mellor 2008; Wu et al. 2011)

$$E = \frac{1}{2}ga^2 = \frac{1}{16}gH_s^2 \tag{4}$$

that can be seen as the sum of the kinetic and the potential wave energies (see Mellor 2003) and

$$E_D = 0 \text{ if } z \neq \hat{\eta} \text{ and } \int_{-h}^{\hat{\eta}+\tilde{\eta}} E_D dz = E/2. \tag{5}$$

Here, x and y are the Cartesian east- and northward directions, respectively, k_x, k_y and k are the x- and y-directed wave numbers and the absolute wave number, respectively, g is the gravitational acceleration, a is the wave amplitude, H_s is the significant wave height, $\hat{\eta}$ is the mean surface elevation and $\tilde{\eta}$ is the surface elevation caused by the wind-generated waves. The terms F_{SS}, F_{SC}, F_{CS} and F_{CC} are defined as follows (see Mellor 2008):

$$F_{SS} \equiv \frac{\sinh k(z+h)}{\sinh kD} \tag{6}$$

$$F_{SC} \equiv \frac{\sinh k(z+h)}{\cosh kD} \tag{7}$$

$$F_{CS} \equiv \frac{\cosh k(z+h)}{\sinh kD} \tag{8}$$

$$F_{CC} \equiv \frac{\cosh k(z+h)}{\cosh kD} \tag{9}$$

The effect of the radiation stress in water waves was first described by Longuet-Higgins and Stewart (1962, 1964) and is calculated as the phase-averaged depth-integrated flux of horizontal momentum caused by a harmonic one-directional wave traveling in the x-direction (see also Longuet-Higgins 1970):

$$\begin{aligned} S_{xx} &= \overline{\int_{-h}^{\zeta} \left(p + \rho u_x^2\right) dz} - \int_{-h}^{0} p_0 dz \\ &= E\left(\frac{2kh}{\sinh 2kh} + \frac{1}{2}\right) \end{aligned} \tag{10}$$

Here, D, ζ, h, p, p_0, ρ and u_x are the total water depth, surface elevation, depth, wave-induced pressure, hydrostatic pressure, water density and particle velocity in the x-direction, respectively. The term ρu_x^2 describes the transport of momentum at a rate u_x per unit time. This net wave-induced momentum flux acts as a 2D stress tensor (see also Moghimi et al. 2013) and the gradients in these stresses act as current-generating forces (e.g. in the x-direction, see Holthuijsen 2007):

$$F_x = -\frac{\partial S_{xx}}{\partial x} - \frac{\partial S_{xy}}{\partial y} \tag{11}$$

This effect is especially obvious inside the surf zone.

The set of equations by Mellor (2008) presented above utilises a depth-dependent radiation stress tensor which can be incorporated in ocean models coupled to wave models. The radiation stress formulation is based on the total mean (Lagrangian) velocity, while Ardhuin et al. (2008b) deal with equations for the current (Eulerian) velocity (see Mellor 2013). Moghimi et al. (2013) reported unrealistic offshore-directed transport for the radiation stress method in regions characterized by rather steep slopes, and Mellor (2013) presents an estimate to test whether linear wave relations (as assumed on the basis of the wave radiation stress derivation) are appropriate in the presence of a sloping bottom. This method is used in Section 6 to test wether the results calculated with the radiation stress method are realistic or not.

In order to provide an adequate representation of an irregular topography vertically, a σ-coordinate system is used. The vertical velocity is placed at the surface of the σ-layer, while all other variables are calculated at the mid-level of a layer. FVCOM allows the user to use either uniform or non-uniform σ-layers.

The salinity and the temperature were set to a constant value of 35 PSU and 10 °C, respectively. This choice might be justified by the fact that during the investigated period in autumn, density gradients in the Wadden Sea show a seasonal minimum (see Wang et al. 2012). The default values for bottom friction and vertical and horizontal mixing were applied.

The 2D third-generation structured-grid surface wave model SWAN (see Booij et al. 1999) was modified by implementing finite-volume algorithms and adding these to the original source code of FVCOM as an unstructured-grid finite-volume version named FVCOM-SWAVE solving the action balance equation (see Qi et al. 2009) for the use in coastal ocean regions with a complex irregular geometry. Second-order upwind-schemes are used in geographical space. The processes of wave growth, quadruplet and triad wave interactions, white capping, wave breaking and bottom friction are included as sink-source terms as also done in the SWAN model and were activated during the coupled model runs. The default conditions for wave energy input and dissipation and for wave propagation were applied. This modelling system can be applied to investigate the influence of wave energy generated by wind along the coast and the resulting wave-induced currents. It should be mentioned that an unstructured-grid version is also available within the SWAN modelling system (see Zijlema 2010). In contrast to the second-order schemes used by FVCOM-SWAVE, first-order implicit Euler schemes in geographical space are adopted to achieve a robust implementation. Zijlema (2010) mentions that the wave action is dictated by source terms and the changes of the energy field in geographical space are relatively weak. Thus, a certain amount of numerical diffusion due to the lower order scheme could be safely tolerated in the numerical scheme for geographic propagation, as its impact on wave parameters is negligible.

3.2 Model topography and surface wind and pressure forcing

The digital topography of the East Frisian Wadden Sea is a combination of high-resolution data provided by the BSH and the NLWKN (Niedersächsischer Landesbetrieb für Wasserwirtschaft, Küsten- und Naturschutz). The topography data for the deeper North Sea were taken from the ETOPO2 (US Department of Commerce, National Oceanic and Atmospheric Administration, National Geophysical Data Center, 2006. 2-minute Gridded Global Relief Data (ETOPO2v2)) data set (see Lettmann et al. 2009).

The coastline was extracted from the commercial software Cruising Navigator distributed by Maptech Inc. and combined with the extracted coastline from the NOAA National Geophysical Data Center (WVS) (ngdc.noaa.gov/mgg/shorelines). The wind and pressure data was provided by the DWD (German Weather Service) with a temporal resolution of 1 h in 2006 and 2 h in 2007.

3.3 Mesh generation

FVCOM does not include a mesh generating system, and a freely available finite element mesh generator called GMSH was therefore used (see Geuzaine and Remacle, 2009). With this tool, the resolution of the mesh can be increased in areas of interest. For this study, the mesh resolution was increased in the area of the tidal inlets between the barrier islands because of the high current velocities known to occur there.

Before a mesh can be generated, a coastline and topography dataset has to be provided by the user. The generated mesh was improved with respect to some empirical quality criteria. The following criteria were applied (see manual given by Chen et al. 2006):

1. The minimum interior angle must be greater than 30°.
2. The maximum interior angle must be less than 130°.

3. The area change of adjacent triangles must be less than a factor of 2.

Figure 4 shows a section of the mesh used for the investigations carried out in this study.

The resolution of the coastline and inside the model area close to the area of interest is 120 m. It is reduced to 300 and 500 m in an intermediate zone and finally to 2000 m in the region close to the boundary of the model. In the tidal channels, the resolution is 50 m in order to sufficiently resolve higher dynamics (see Fig. 4).

This mesh is one-way coupled to the North Sea Model, which has also been generated with GMSH. This model has a resolution of 500 m in the area of the East Frisian Wadden Sea and a reduced resolution down to 6000 m in deeper areas.

Due to the different maximum resolutions, different time steps for the two model setups were applied. FVCOM-SWAVE was used in a non-stationary mode with a time step of 300 s for the North Sea model and a time step of 10 s for the Wadden Sea model. For the hydrodynamic part of FVCOM, a time step of 10 s for the North Sea model and a time step of 2 s for the Wadden Sea model were used.

The computations were performed on the cluster of the North-German Supercomputing Alliance (Norddeutscher Verbund zur Förderung des Hoch- und Höchstleistungsrechnens—HLRN) and the cluster High-End Computing Resource Oldenburg (HERO), funded by the Deutsche Forschungsgemeinschaft (DFG) and the Ministry of Science and Culture (MWK) of the State of Lower Saxony, Germany.

3.4 Surface and wave forcing at the open boundaries

The modelling system FVCOM-SWAVE allows the model to be forced at the open boundary using a predetermined surface elevation and/or wave conditions. For the surface elevation at the three open boundaries (see Fig. 1) of the North Sea model, the output of the global tide model FES2004 (Finite Element Solution 2004) was used. FES2004 was produced by Legos and CLS Space Oceanography Division and distributed by Aviso, with support from CNES (www.aviso.oceanobs.com) (see Lyard et al. 2006). The surface elevation is affected by the inverse barometer effect, such that a change of 1 hPa will result in a change of 1 cm in surface elevation. This correction was applied in order to add surge levels to the tidal levels in the FES2004 output data over the whole hindcast periods using the pressure data that was extracted from the DWD dataset and interpolated on the boundary nodes of the unstructured grid of the North Sea model setup.

Parametric sea state variables provided by the global wave model WW3 (in 2006 see Chawla et al. (2012) and in 2007 see Rascle and Ardhuin (2013)) were used as the wave boundary conditions over the two hindcast periods for the North Sea setup. The Wadden Sea model is one-way nested in the North Sea model, thus providing the surface elevation and wave conditions for the open boundary forcing of

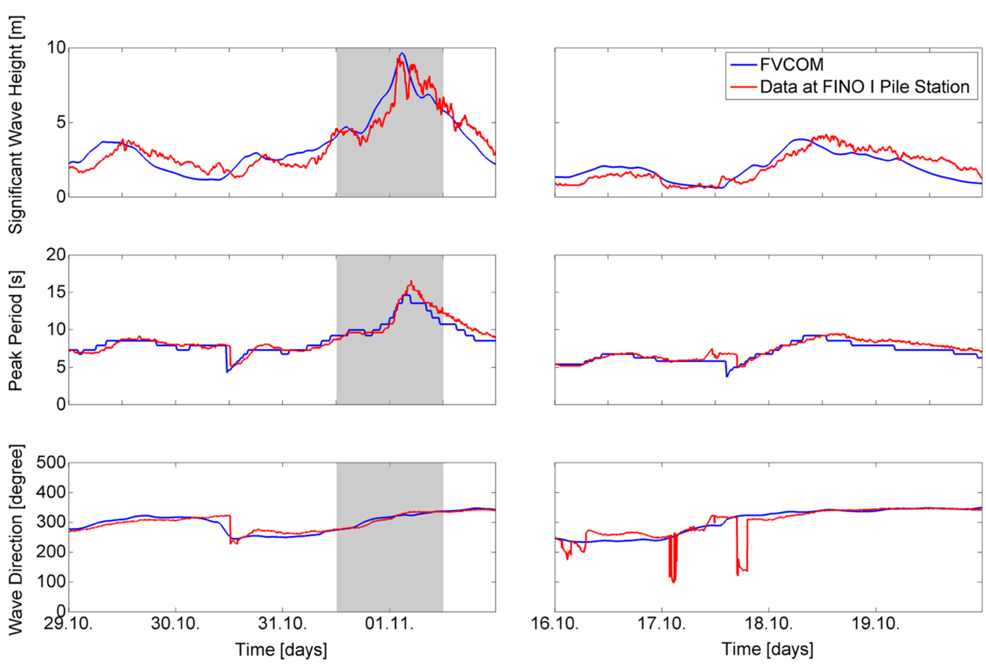

Fig. 5 Observed and modelled significant wave heights H_s, peak periods T_p and wave directions θ at the FINO I pile station. *Left panel*: 4 days in the winter period of 2006 (including the *grey colored time* frame of storm surge Britta). *Right panel*: 4 days in October 2007 with moderate wind conditions

the highly resolved model. The peak period at the boundary had to be smoothed to guarantee a stable model run. In FVCOM version 3.1.4, it is only possible to force the model using variables such as the significant wave height, the peak period and the wave direction. Therefore, these variables and not the 2D wave spectrum are used as model forcing parameters.

4 Validation and comparison of the model results

For model validation purposes, two time periods in 2006 and 2007 were analysed for the North Sea and the Wadden Sea model. In 2006, a major storm event called Britta occurred in the North Sea and is used to test the ability of the model setups to reproduce reliable results during an extreme event. During the 2007 period, moderate atmospheric conditions prevailed over the southern North Sea.

Figure 5 shows the calculated and observed significant wave height, peak period and wave direction, whereas in Fig. 6, the surface elevation in Oct./Nov. 2006 and Oct. 2007 at the FINO I pile station and ICBM pile station (see Fig. 1) are shown. The mean significant wave height during the period in 2007 was around 3 m, but during the storm event in 2006, the significant wave height increased to > 9 m. For this latter event, the model reproduces the observed significant wave height, peak period and wave direction reasonably well. It can also be seen that in 2006 and 2007, the main wave directions were N-NW, and that the main peak period was about 7 s in 2007, whereas it reached 14 s during the 2006 storm event.

In 2007, the modelled results seem to reproduce the characteristics of the observed surface elevation well with a good agreement in the phase of the tidal signal. In 2006, the peak of the surface elevation during the storm event is underestimated by the model, but again the model and the observed values are in phase most of the time.

In Fig. 7, the simulated velocities from the North Sea model are compared with the observations obtained during a ship cruise on a fixed position in October 2007. The model underestimates the velocities during the ebb phase and the process of the upcoming low tide takes longer than during the measurement. Again, the modelled and observed phases of the tidal signal match well. A vertical velocity profile at the ICBM pile station (see Fig. 1) can be seen in Fig. 8. The North Sea model clearly underestimates the current velocity, but the Wadden Sea model shows good overall agreement with the observations. Obviously, some short-periodic oscillations in the data are either noise or physical oscillations which the model does not resolve.

5 Wave energy flux

Water particles do not travel with the speed of a propagating wave and stay close to their original position. Therefore, almost no mass is transported by a traveling wave train. However, energy is transferred by a wave in the direction of propagation. In the region of the East Frisian Wadden

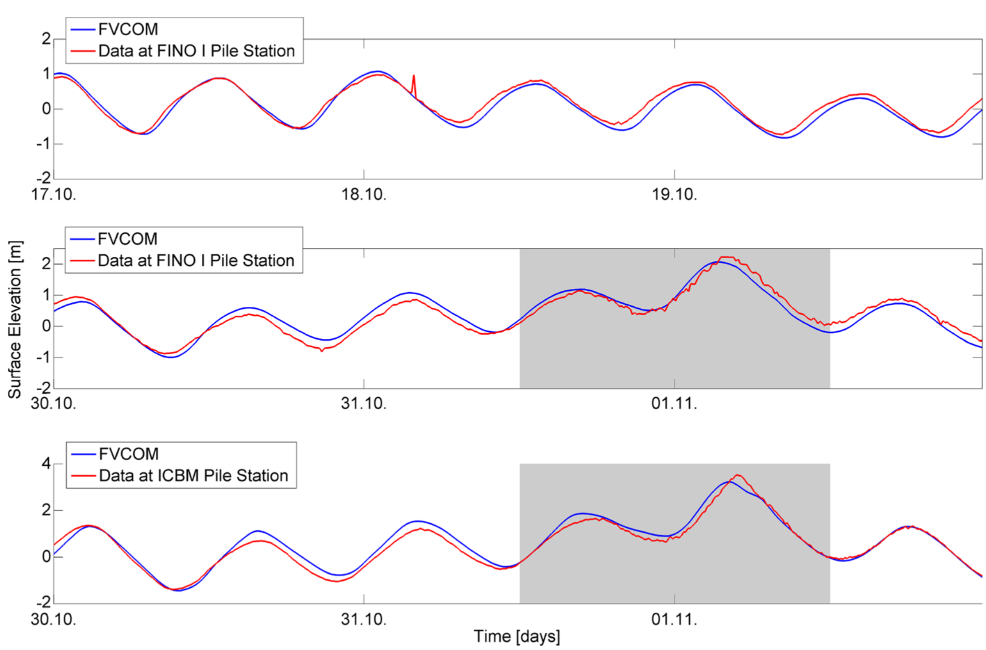

Fig. 6 Observed and modelled surface elevations at the FINO I and the ICBM pile station. The *top plot* depicts the surface elevation calculated with the North Sea setup at FINO I over the period 17–20.10.2007. The *middle plot* shows the calculated surface elevation over the period from 30.10.-02.11.2006 and includes the storm surge Britta (*grey* colour). The *bottom plot* depicts the surface elevation during the storm Britta calculated with the Wadden Sea setup at the ICBM pile station

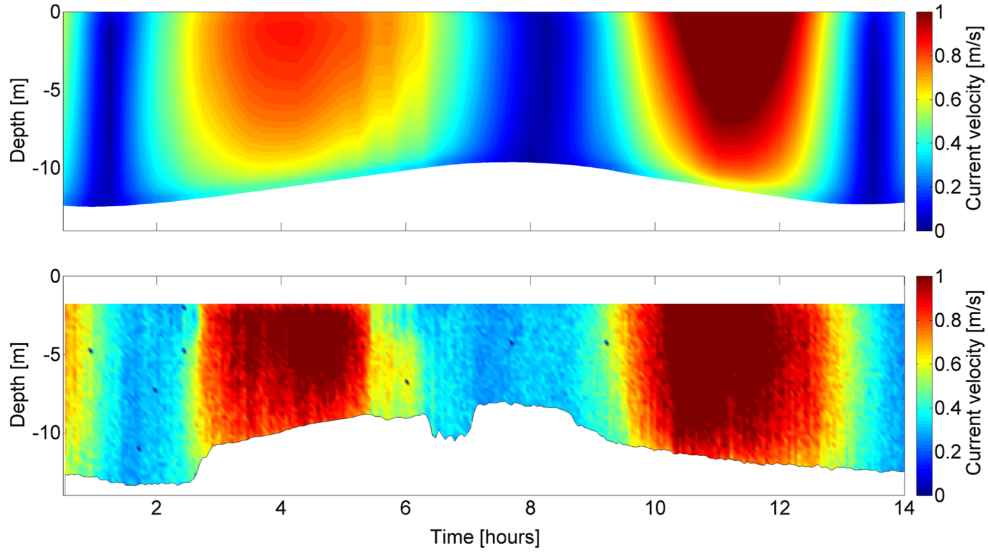

Fig. 7 Modelled (*top panel*) and observed (*bottom panel*) current velocities of the North Sea model at a fixed position between two barrier islands. The measurements started at 00:00:00 UTC on 17.10.2007

Sea, the chain of barrier islands acts like a natural protection of the German north-west coast and 'absorbs' most of the energy. Here, the amount of wave energy or wave energy flux is calculated to estimate the impact on the barrier islands during a storm event and a time period without significant storms.

The wave energy flux of one wave is defined as the product of energy density and the group velocity of the waves (see Cornett and Zhang, 2008). To take the whole wave train into account, this product has to be integrated over all wave frequencies and directions:

$$P = \rho g \int_0^{2\pi} \int_0^{\infty} c_g\,(f, h)\, S\,(f, \Theta)\, df\, d\Theta \tag{12}$$

Here, $S\,(f, \Theta)$ is the 2D wave spectrum, $c_g\,(f, h)$ is the group velocity, f is the wave frequency and Θ the wave direction. The group velocity of every single wave inside a wave train can be calculated as (see Cornett and Zhang 2008; Holthuijsen 2007)

$$c_g\,(f, h) = \frac{1}{2}\left[1 + \frac{2kD}{\sinh 2kD}\right]\sqrt{\frac{g}{k}\tanh kD} \tag{13}$$

where kD can be estimated using an approximation given by Fenton and McKee (1990) (see also Holthuijsen 2007). Since the energy flux is not yet implemented in the output of the model, an approximation of the wave energy flux per unit wave crest length produced by a wave train of irregular waves in any water depth can be estimated from the wave energy (see Eq. 4), the peak wave period T_p and the local water depth as

$$P \approx \frac{1}{16}\rho g H_s^2 c_g \left(\frac{1}{\alpha_E T_p}, D\right) \tag{14}$$

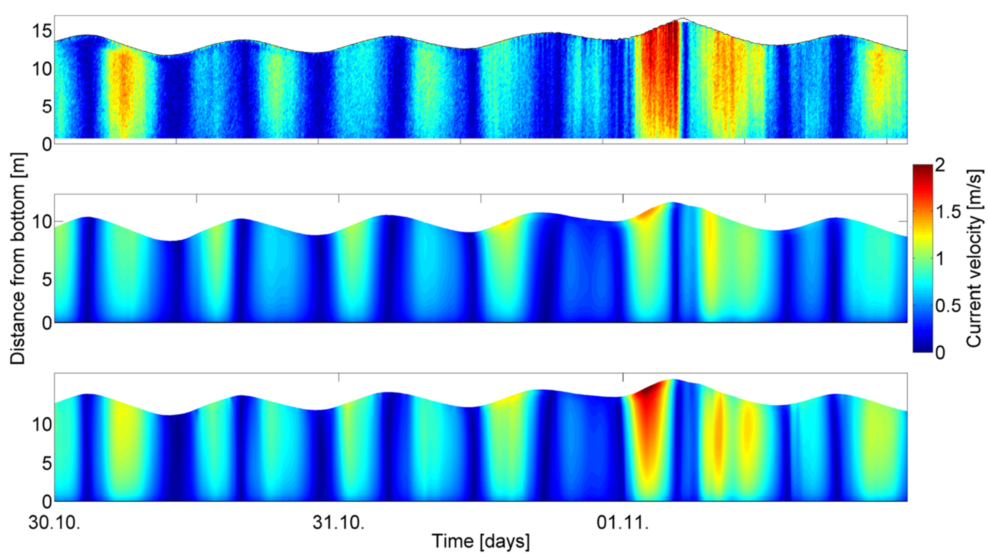

Fig. 8 Observed and modelled current velocity at the ICBM pile station between two barrier islands starting on the 30.10.2006 and ending on the 02.11.2006. The *top panel* shows the observations, whereas the *middle and lower panels* show the results of the North Sea and Wadden Sea models, respectively

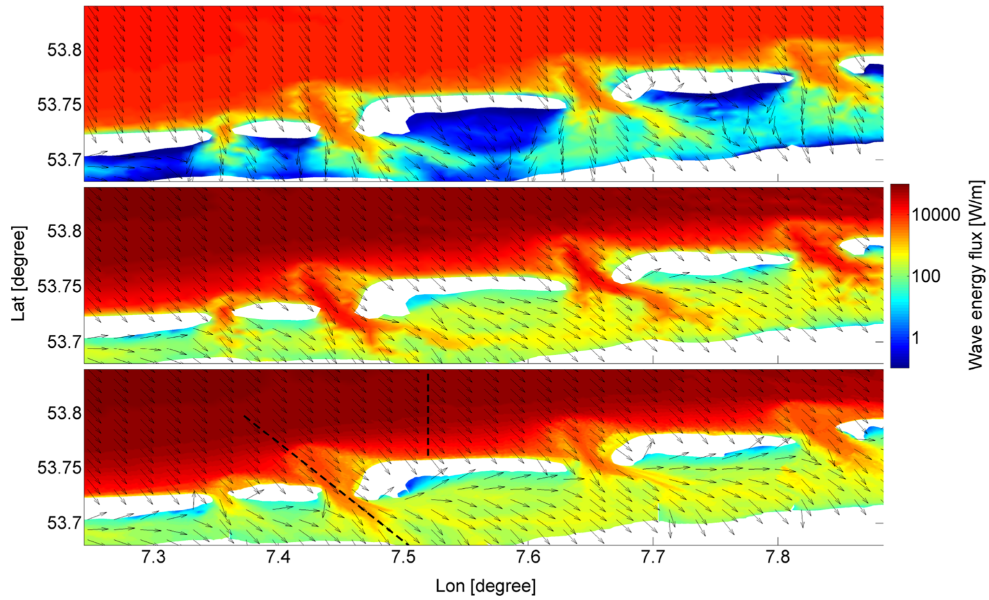

Fig. 9 Modelled mean wave energy flux. The figure at the top (North Sea model) shows the mean wave energy flux in the period from 16–20.10.2007. The middle (North Sea model) and bottom (Wadden Sea model) figures depict the period from 30.10.-02.11.2006 and include the storm surge Britta. The *arrows* have been interpolated onto an uniform grid and normalised to 1

where $c_g\left(\frac{1}{\alpha_E T_p}, D\right)$ is the group velocity of a wave with a period of $\alpha_E T_p$. The parameter α_E is a coefficient that depends on the shape of the wave spectrum and shifts the peak period to lower periods. If a sea state is dominated by waves from a single source and the spectrum is uni-modal, Cornett and Zhang (2008) suggest a value of $\alpha_E \approx 0.9$, which was also used here.

The resulting mean wave energy flux can be seen in Fig. 9 for the two different time periods in 2006 and 2007. In 2006, a mean wave energy of about 90 kW/m approaches the coast. In 2007, less energy is transported by the waves, but in all three cases, the barrier islands absorb most of the wave energy. The influence of the ebb-tidal delta in front of the inlet can also be identified.

Figure 10 shows the profile of the maximum daily mean and the mean wave energy in the period from 30.10. –02.11.2006 interpolated on a section in front of the coast of a barrier island and along a tidal inlet (see Fig. 9). It can be seen that the maximum daily mean wave energy flux can reach up to 200 kW/m in front of the coast during the storm event, a value quite similar to the 160 kW/m found by Pleskachevsky et al. (2009). During the time before the peak of the storm event, the significant wave height was overestimated by the North Sea model (see Fig. 5). After

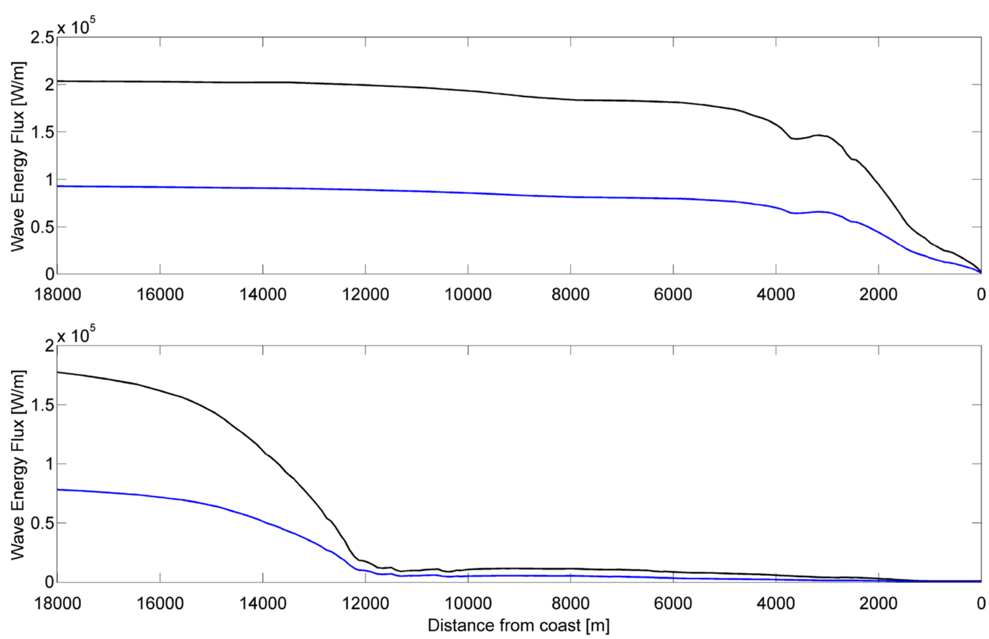

Fig. 10 Profile of the mean wave energy flux calculated by the Wadden Sea model. The maximum daily mean (*black line*) and the mean wave energy flux (*blue line*) in the period from 30.10.-02.11.2006 are shown. The upper plot depicts the section in front of the barrier island Langeoog. The plot at the bottom shows the wave energy flux along a tidal inlet. The position of the sections are indicated with *dashed black lines* in the bottom panel of Fig. 9

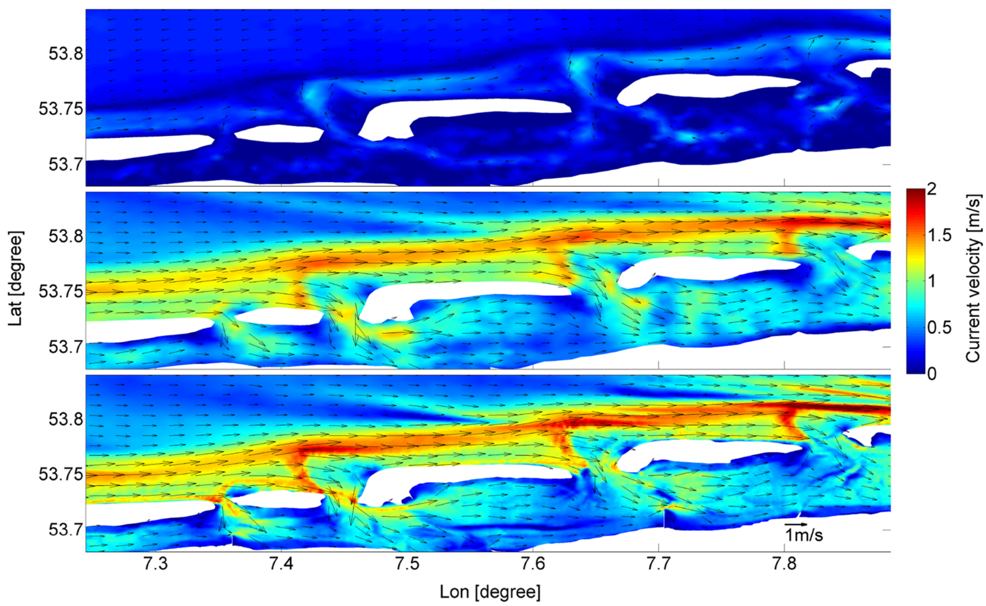

Fig. 11 Depth-averaged current velocity. The plot at the top (North Sea model) shows the depth-averaged current velocity at 08:00:00 UTC on 18.10.2007. The middle (North Sea model) and bottom (Wadden Sea model) plots represent the time slice at 01:00:00 UTC on 01.11.2006 during the storm surge Britta. The *arrows* have been interpolated onto an uniform grid

the storm event, the model results fail to reproduce some secondary peaks and show a stronger decrease in significant wave height than the observational data covering a longer period compared to the results prior to the storm event. Thus, the influence of the storm event on the averaged wave energy flux might be underestimated and the real energy flux might be even higher. During the moderate situation in 2007, a similar behaviour can be recognised. The quality of the results in the area of the tidal basins strongly depends on the bathymetric data. Intertidal channels might be missing due to interpolation procedures, and this might decrease the significant wave height and, consequently, the wave energy flux in certain areas.

The wave energy flux begins to strongly decrease at about 4 km offshore the barrier island Langeoog. Along the tidal inlet, it decreases rapidly as the ebb-tidal delta is crossed to a value of less than 10 % of the value in front of the barrier islands as already pointed out by Krögel and Flemming (1998).

6 Radiation stress effects

Higher waves will result in higher wave energy and thus generate higher radiation stress gradients. When approaching the coast this effect will contribute to increased current

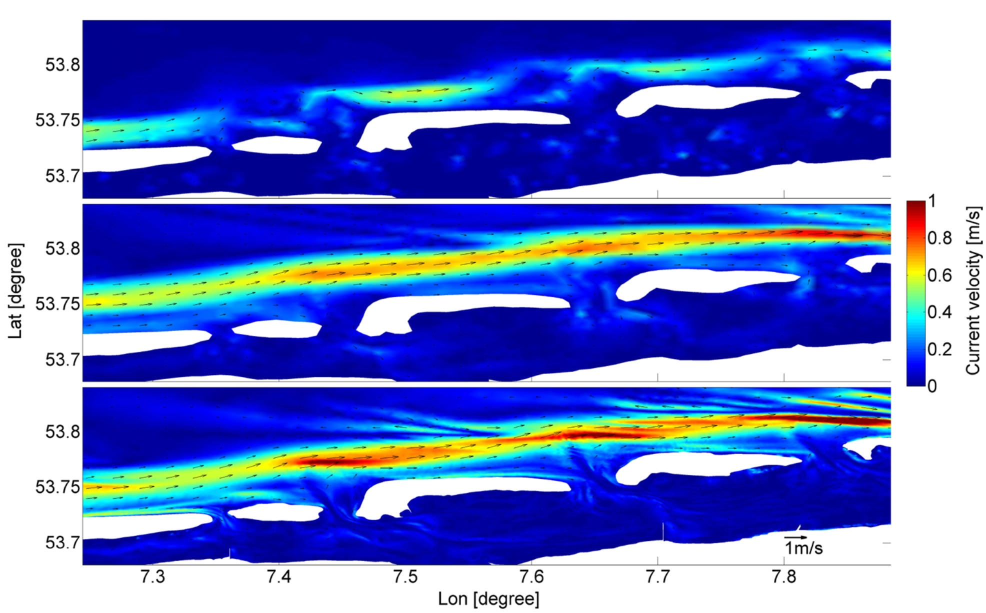

Fig. 12 Modelled difference in depth-averaged current velocity due to wave-current interaction. The plot at the top (North Sea model) shows the difference in depth-averaged current velocity at 08:00:00 UTC on 18.10.2007. The middle (North Sea model) and bottom (Wadden Sea model) plots represent the time slice at 01:00:00 UTC on 01.11.2006 during the storm surge Britta. The depth-averaged current velocity is calculated as the difference of two model runs with and without the wave model coupled to the hydrodynamic model. The *arrows* have been interpolated onto an uniform grid

velocities in the coastal area. Especially during a storm event, high waves occur and generate strong longshore currents (see Pleskachevsky et al. 2009). As mentioned above, Mellor (2003) and Mellor (2008) derived a set of equations that can be used as governing equations for an ocean model such as FVCOM. In these equations, a coupling between waves and currents is achieved by implementing the gradients of radiation stresses as a force acting on the current field. The effect of the current field on the wave is included in the action balance equation. The depth-averaged Doppler velocity is approximated from the current calculated with input of the hydrodynamic and wave model as (see Mellor 2008 and Wu et al. 2011)

$$u_{A\alpha} = kD \cdot \int_{-1}^{0} U_\alpha \left[\left(F_{CS} F_{CC} + F_{SS} F_{SC} \right) / 2 + F_{CS} F_{SS} \right] d\sigma \ . \quad (15)$$

Here, α refers to a horizontal coordinate, U_α is the velocity of the ambient current and σ is the σ-coordinate.

The North Sea model setup and the Wadden Sea model setup of FVCOM (one-way coupled to the North Sea model) were used to calculate the wave-generated velocities along the East Frisian Coast. In Fig. 11, the depth-averaged current velocity during the storm surge event is shown. In front of the barrier island Langeoog (see Fig. 1), the longshore currents reach values around 1.5 m/s and in the area of the ebb-tidal deltas it increases to 2 m/s. The wave-induced current velocity is calculated by the difference between a model run with and without the wave model coupled to the hydrodynamic model. In Fig. 12, it can be seen that during the storm period in 2006, the strongest purely wave-generated longshore currents reached values up to around 0.7 m/s in the North Sea model and around 1.0 m/s in the Wadden Sea model. In conjunction with Fig. 11, this means that 50 % of the overall depth-averaged current velocity of the longshore currents in front of the barrier islands are generated by wave-current interactions. During 2007, no significant storm surges occurred and the highest longshore currents reached maximum values around 0.6 m/s.

As summarised above, the radiation stress method was criticised in several papers. Offshore currents are suspected to be overestimated by this method in the presence of steep slopes. In Fig. 13, the vertical structure of the difference of the u- and the v-component of the current between a model run with and without waves coupled to the hydrodynamic model along a cross-section in front of the barrier island Langeoog (cf. Fig. 9) can be seen. Offshore-directed currents can be recognised here, but it is not clear if these effects are caused by the implementation of the radiation stress method. In Fig. 12, it can be seen that the longshore current in front of the barrier islands is directed slightly offshore in a north-easterly direction. In fact, the currents follow the structure of the bathymetry as is shown in Fig. 2. In this region, a strong reduction of the significant wave height occurs (see also Fig. 14) which is responsible for the initiation of the longshore currents. Thus, the offshore direction of the currents might be a consequence of the local structure of the bathymetry and resulting effects of the wave-current interactions.

It should be mentioned that in some regions, the longshore currents are underestimated by both formulations (vortex force and radiation stress), as shown by Moghimi et al. (2013). This means that the longshore currents presented here might be underestimated in certain regions. In Fig. 13, it is also shown that the velocity of the longshore current induced by the waves reaches values up to

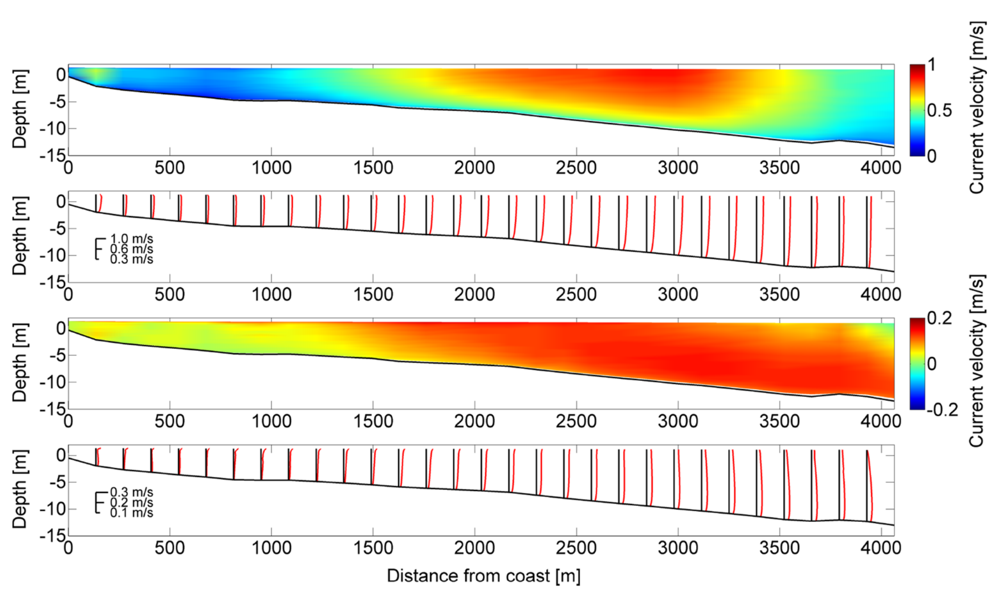

Fig. 13 Cross-section of the modelled difference of the u-component and the v-component of the current between two model runs with and without the wave model coupled to the hydrodynamic model at 01:00:00 UTC on 01.11.2006, during the storm surge Britta (Wadden Sea model). The two upper panels depict the velocity component u and the two bottom ones the velocity component v. The position of the cross-section in front of the barrier island Langeoog is shown in Fig. 9

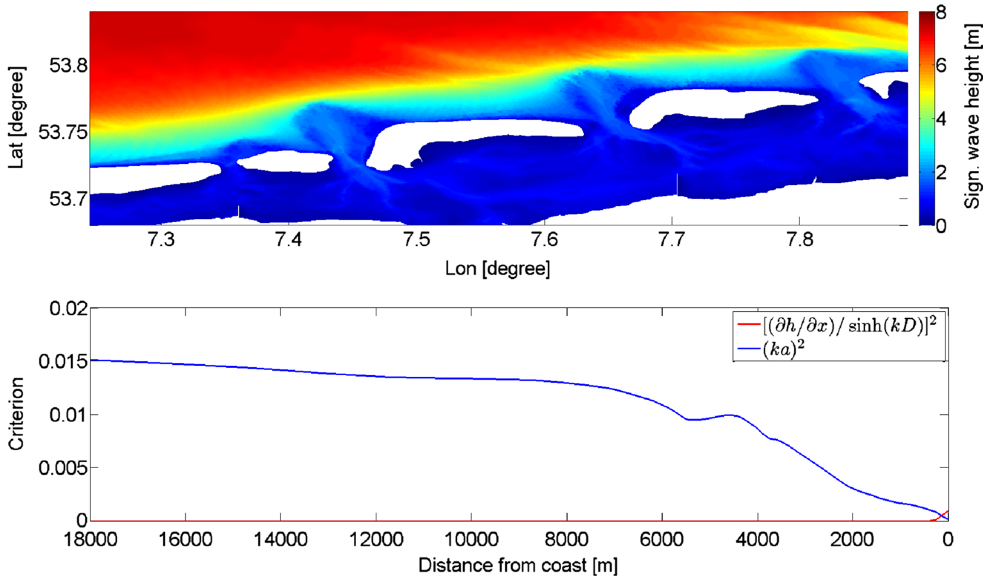

Fig. 14 Significant wave height (*top panel*) calculated by the Wadden Sea model at 01:00:00 UTC on 01.11.2006, during the storm surge Britta and visualisation of the criterion (*bottom panel*) proposed by Mellor (2013). The position of the cross-section in front of the barrier island Langeoog is shown in Fig. 9

1 m/s during the storm event. This means the additional current due to the waves is of about the same magnitude as the ambient current, as also reported from the Catalan coast (see Bolanos et al. 2008) and the North Frisian island Sylt (see Pleskachevsky et al. 2009).

Mellor (2013) proposed a criterion to check if it is appropriate to use the radiation stress method in the presence of a bottom slope. He states that the term $[(\partial h/\partial x)/\sinh kD]^2$, which includes the bottom slope, should be small and of the order $(ka)^2$. Assuming a Rayleigh wave height distribution $a = \frac{1}{2}H_{rms}$ can be calculated using the significant wave height H_s (see Holthuijsen 2007):

$$H_{rms} = \frac{1}{2}\sqrt{2}H_s \quad (16)$$

In Fig. 14, it is shown that along the cross-section in front of the barrier island Langeoog (see Fig. 9), this criterion is satisfied even close to the coast, where offshore directed currents caused by the implementation of the radiation stress method (see Fig. 13) might also occur. Only directly at the coastline, the criterion is no longer satisfied, but this is negligible because the main dynamics occur far away from this region (see Fig. 13).

The wave-current interactions also influence the surface elevation in the East Frisian Wadden Sea area. Figure 15 shows the surface elevation during the storm surge Britta and the residual currents in the period from 31.10.-01.11.2006. The waves produce an increased surface elevation of around 0.3 m over most of the tidal flats. The overall

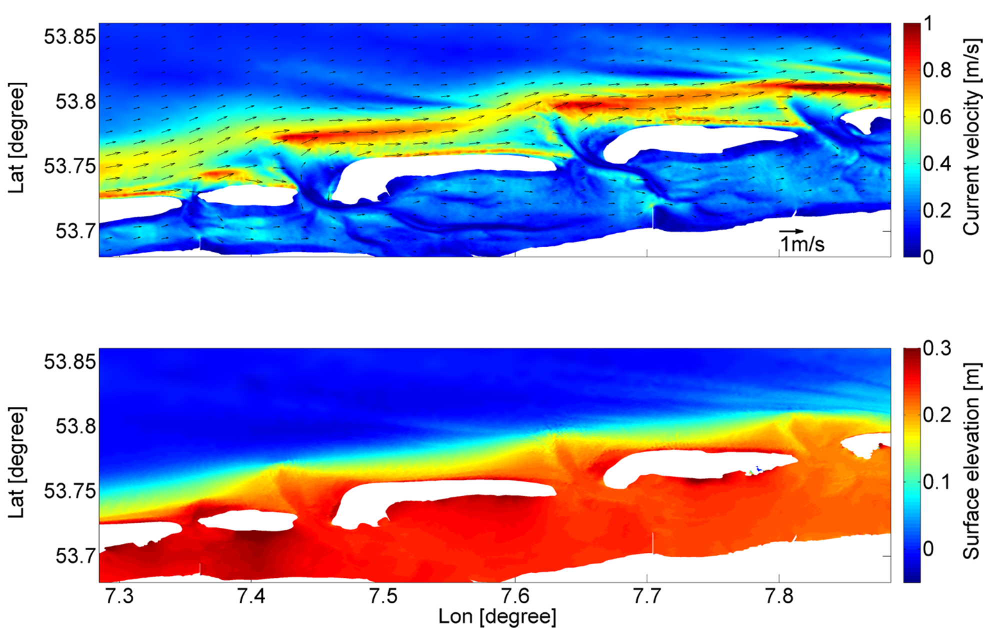

Fig. 15 Modelled overall depth-averaged residual current and the difference in surface elevation due to wave-current interaction (Wadden Sea model). The *upper panel* shows the residual currents in the period from 31.10.-01.11.2006. Again, the *arrows* have been interpolated onto an uniform grid. The *bottom picture* depicts the difference in surface elevation between two model runs with and without the wave model applied during the storm event Britta at 01:00:00 UTC on 01.11.2006

maximum residual current during the storm event is around 1 m/s.

7 Summary

An unstructured-grid ocean model with a North Sea and a Wadden Sea model setup has been tested and validated for a storm and a moderate weather situation in 2006 and 2007, respectively. The Wadden Sea model is one-way coupled to the North Sea model. The high-resolution Wadden Sea model shows a better performance in predicting current velocities compared to the coarser North Sea model, indicating energy diffusion in the coarser model. However, the North Sea model setup also reproduces the structure of the wave-induced longshore currents. The Wadden Sea model setup can be used for the investigation of small-scale processes around the barrier island system of the East Frisian Wadden Sea.

A first estimate of the wave-induced energy flux has been calculated, showing a high energy flux under storm conditions and the ability of the barrier island system to absorb most of the energy, as previously postulated by Krögel and Flemming (1998). Some of the energy also enters the inlet and is dissipated while traveling through the channel, also contributing erosion potential in this area.

Residual longshore currents that were expected to occur under storm conditions could be reproduced by implementing wave-current interaction mechanisms in the model. As direct observations of longshore currents in this region during storm events do not exist, these results are a first approach to estimate the magnitude of this effect in the East Frisian barrier island system. This effect may play a major role in sediment transport and should be a focus of further investigations in future studies. The method presented by Mellor (2003, 2008), which was used to couple the surface wave and the hydrodynamic model part, is still under discussion and further development. Thus, the wave-induced longshore currents estimated by the model have to be tested by future model runs implementing newer formulations of the radiation stress or alternative approaches such as the vortex force method. In Section 6, a criterion proposed by Mellor (2013) was used to test whether the application of the radiation stress method in this region will give reasonable results.

Another subject of future work should be the realisation of long-term runs and the implementation of a variable temperature and salinity distribution in the model setup.

Acknowledgements The study was supported by the Ministry for Science and Culture of Lower Saxony within the network KLIFF—climate impact and adaption research in Lower Saxony, the initiative Earth Science Knowledge Platform (ESKP) operated by the Helmholtz Association and the North-German Supercomputing Alliance (Norddeutscher Verbund zur Förderung des Hoch- und Höchstleistungsrechnens—HLRN). The authors like to thank Changsheng Chen and the other developers of the ocean modelling suite FVCOM for providing the source code of the ocean model, Reinhard Leidl and staff at the cluster HERO (High-End Computing Resource Oldenburg), funded by the Deutsche Forschungsgemeinschaft (DFG) and the Ministry of Science and Culture (MWK) of the State of Lower Saxony, Germany and the people at the BSH, Federal Maritime and Hydrographic Agency of Germany. The authors also like to thank Oliver Bleich and Steffen Rettig for extracting and optimising coastline data and Burghard Flemming for advice on prescriptive linguistics.

References

Aiki H, Greatbatch RJ (2012) Thickness-weighted mean theory for the effect of surface gravity waves on mean flows in the upper ocean. J Phys Oceanogr 42:725–747

Aiki H, Greatbatch RJ (2013) The vertical vtructure of the surface wave radiation stress for circulation over a sloping bottom as given by thickness-weighted-mean theory. J Phys Oceanogr 43(1):149–164

Aiki H, Greatbatch RJ (2014) A new expression for the form stress term in the vertically Lagrangian mean framework for the effect of surface waves on the upper-ocean circulation. J Phys Oceanogr 44(1):3–23

Andrews DG, McIntyre ME (1978) An exact theory of nonlinear waves on a Lagrangian-mean flow. J Fluid Mech 89:609–646

Ardhuin F, Jenkins AD, Belibassakis KA (2008a) Comments on The Three-Dimensional Current and Surface Wave Equations. J Phys Oceanogr 38(6):1340–1350

Ardhuin F, Rascle N, Belibassakis KA (2008b) Explicit wave-averaged primitive equations using a generalized Lagrangian mean. Ocean Model 20(1):35–60

Bartholomä A, Kubicki A, Badewien TH, Flemming BW (2009) Suspended sediment transport in the German Wadden Sea-seasonal variations and extreme events. Ocean Dyn 59(2):213–225

Bennis AC, Ardhuin F (2011) Comments on "The depth-dependent current and wave interaction equations: A Revision". J Phys Oceanogr 41(10):2008–2012

Benoit M, Marcos F, Becq F (1996) Development of a third generation shallow-water wave model with unstructured spatial meshing. In: Proceedings of the 25th International Conference on Coastal Engineering, ASCE, Orlando, pp. 465–478

Bolanos R, Osuna P, Wolf J, Monbaliu J, Sanchez-Arcilla A (2008) The POLCOMS-WAM Wave-Current Interaction Model: development and performance in the NW Mediterranean. In: Guedes Soares C, Kolev PK (eds) Maritime industry, ocean engineering and coastal resources: proceedings of the 12th International congress of the international maritime association of the Mediterranean, (IMAM 2007), Varna, Bulgaria, 2-6 September 2007. London, Taylor Francis, 685–691

Booij N, Ris RC, Holthuijsen LH (1999) A third-generation wave model for coastal regions: 1. Model description and validation. J Geophys Res 104(C4):7649–7666

Brown JM, Bolaños R, Wolf J (2011) Impact assessment of advanced coupling features in a tide-surge-wave model, POLCOMS-WAM, in a shallow water application. J Mar Syst 87(1):13–24

Brown JM, Bolaños R, Wolf J (2013) The depth-varying response of coastal circulation and water levels to 2D radiation stress when applied in a coupled wave-tide-surge modelling system during an extreme storm. Coast Eng 82:102–113

Chawla A, Spindler D, Tolman H (2012) 30 Year Wave Hindcasts using WAVEWATCH III with CFSR winds–Phase 1. Tech. Note 302, NOAA/NWS/NCEP/MMAB, 12 pp

Chen C, Beardsley RC, Cowles G (2006) An unstructured grid, finite-volume coastal ocean model, FVCOM user manual 2nd edn. SMAST/UMASSD Tech. Rep. 06-0602, 315 pp, School for Marine Science and Technology. University of Massachusetts-Dartmouth, New Bedford. MA

Chen C, Liu H, Beardsley RC (2003) An unstructured grid, finite-volume, three-dimensional, primitive equations ocean model: application to coastal ocean and estuaries. J Atmos Oceanic Technol 20(1):159–186

Cornett A, Zhang J (2008) Nearshore Wave Energy Resources, Western Vancouver Island, B.C., Technical Report CHC-TR-51, Canadian Hydraulics Centre

Dastgheib A, Roelvink JA, Wang ZB (2008) Long-term process-based morphological modeling of the Marsdiep Tidal Basin. Mar Geol 256(1–4):90–100

Dissanayake DMPK, Roelvink JA, van der Wegen M (2009) Modelled channel patterns in a schematized tidal inlet. Coastal Eng 56 (11–12):1069–1083

Fenton JD, McKee WD (1990) On calculating the lengths of water waves. Coastal Eng 14(6):499–513

Flemming BW, Bartholomä A (1997) Response of the Wadden Sea to a rising sea level: a predictive empirical model. Dtsch Hydrogr Z 49(2–3):343–353

Flemming BW, Delafontaine MT (1994) Biodeposition in a juvenile mussel bed of the East Frisian Wadden Sea (Southern North Sea). Neth J Aquat Ecol 28(3–4):289–297

Geuzaine C, Remacle JF (2009) GMSH: a three-dimensional finite element mesh generator with built-in pre- and post-processing facilities. Int J Numer Meth Eng 79(11):1309–1331

Holthuijsen LH (2007) Waves in oceanic and coastal waters. Cambridge University Press

Krögel F, Flemming BW (1998) Evidence for temperature-adjusted sediment distributions in the back-barrier tidal flats of the East Frisian Wadden Sea (southern North Sea). In: C R Alexander et al. (eds) (1998) Tidalites: processes & products. SEPM Special Publication, no. 61. SEPM, Tulsa, pp. 31–41

Lane EM, Restrepo JM, McWilliams JC (2007) Wave-current interaction: a comparison of radiation stress and vortex-force representations. J Phys Oceanogr 37(5):1122–1141

Lettmann KA, Wolff J-O, Badewien TH (2009) Modeling the impact of wind and waves on suspended particulate matter fluxes in the East Frisian Wadden Sea (southern North Sea). Ocean Dyn 59(2):239–262

Loewe P (2009) System Nordsee—Zustand 2005 im Kontext langzeitlicher Entwicklungen. Berichte des Bundesamtes für Seeschifffahrt und Hydrographie 44

Longuet-Higgins MS (1970) Longshore currents generated by obliquely incident sea waves, 1. J Geophys Res 75(33):6778–6789

Longuet-Higgins MS, Stewart RW (1962) Radiation stress and mass transport in gravity waves, with application to 'surf beats'. J Fluid Mech 13(4):481–504

Longuet-Higgins MS, Stewart RW (1964) Radiation stresses in water waves: a physical discussion with applications. Deep-Sea Res 11:529–562

Lyard F, Lefevre F, Letellier T, Francis O (2006) Modelling the global ocean tides: modern insights from FES2004. Ocean Dyn 56 (5–6):394–415

Mellor G (2003) The three-dimensional current and surface wave equations. J Phys Oceanogr 33(9):1978–1989

Mellor G (2005) Some consequences of the three-dimensional current and surface equations. J Phys Oceanogr 35(11):2291–2298

Mellor GL (2008) The depth-dependent current and wave interaction equations: a revision. J Phys Oceanogr 38(11):2587–2596

Mellor G (2011a) Wave radiation stress. Ocean Dyn 61(5):563–568

Mellor G (2011b) Corrigendum J Phys Oceanogr 41(7):1417–1418

Mellor G (2011c) Reply J Phys Oceanogr 41(10):2013–2015

Mellor G (2013) Waves, circulation and vertical dependance. Ocean Dyn 63(4):447–457

Mellor GL, Yamada T (1982) Development of a turbulence closure model for geophysical fluid problems. Rev Geophys 20(4): 851–875

Moghimi S, Klingbeil K, Gräwe U, Burchard H (2013) A direct comparison of a depth-dependent radiation stress formulation and a vortex force formulation within a three-dimensional coastal ocean model. Ocean Model 70:132–144

Osuna P, Monbaliu J (2004) Wave-current interaction in the southern North Sea. J Mar Sys 52(1–4):65–87

Phillips OM (1977) The dynamics of the upper ocean. Cambridge University Press

Pleskachevsky A, Eppel DP, Kapitza H (2009) Interaction of waves, currents and tides, and wave-energy impact on the beach area of Sylt Island. Ocean Dyn 59(3):451–461

Qi J, Chen C, Beardsley RC, Perry W, Cowles GW, Lai Z (2009) An unstructured-grid finite-volume surface wave model (FVCOM-SWAVE): implementation, validations and applications. Ocean Model 28(1–3):153–166

Rascle N, Ardhuin F (2013) A global wave parameter database for geophysical applications. Part 2: model validation with improved source term parameterization. Ocean Model 70: 174–188

Reuter R, Badewien TH, Bartholomä A, Braun A, Lübben A, Rullkötter J (2009) A hydrographic time series station in the Wadden Sea (southern North Sea). Ocean Dyn 59 (2):195–211

Roland A, Ardhuin F (2014) On the developments of spectral wave models: numerics and parameterizations for the coastal ocean. Ocean Dyn 64(6):833–846

Santamarina Cuneo P, Flemming BW (2000) Quantifying concentration and flux of suspended particulate matter through a tidal inlet of the East Frisian Wadden Sea by acoustic Doppler current profiling. In: B W Flemming et al. (eds) Muddy Coast Dynamics and Resource Management. Proceedings in Marine Science, vol. 2. Elsevier, Amsterdam, pp.39–52

Smagorinsky J (1963) General circulation experiments with the primitive equations I. The basic experiment. Mon Wea Rev 91(3): 99–164

Stanev EV, Flöser G, Wolff J-O (2003a) First- and higher-order dynamical controls on water exchanges between tidal basins and the open ocean. A case study for the East Frisian Wadden Sea. Ocean Dyn 53(3):146–165

Stanev EV, Wolff J-O, Burchard H, Bolding K, Flöser G (2003b) On the circulation in the East Frisian Wadden Sea: numerical modeling and data analysis. Ocean Dyn 53 (1):27–51

Stanev EV, Wolff J-O, Brink-Spalink G (2006) On the sensitivity of the sedimentary system in the East Frisian Wadden Sea to sea-level rise and wave-induced bed shear stress. Ocean Dyn 56(3–4): 266–283

Stanev EV, Brink-Spalink G, Wolff J-O (2007a) Sediment dynamics in tidally dominated environments controlled by transport and turbulence: a case study for the East Frisian Wadden Sea. J Geophys Res 112(C4)

Stanev EV, Flemming BW, Bartholomä A, Staneva JV, Wolff J-O (2007b) Vertical circulation in shallow tidal inlets and back-barrier basins. Cont Shelf Res 27(6):798–831

Stanev EV, Grayek S, Staneva J (2008) Temporal and spatial circulation patterns in the East Frisian Wadden Sea. Ocean Dyn 59(2):167–181

Staneva J, Stanev EV, Wolff J-O, Badewien TH, Reuter R, Flemming B, Bartholomä A, Bolding K (2009) Hydrodynamics and sediment dynamics in the German Bight. A focus on observations and numerical modelling in the East Frisian Wadden Sea. Cont Shelf Res 29(1):302–319

Thornton EB, Guza RT (1986) Surf Zone Longshore Currents and Random Waves: field data and models. J Phys Oceanogr 16(7):1165–1178

Timmermann R, Danilov S, Schröter J, Böning C, Sidorenko D, Rollenhagen K (2009) Ocean circulation and sea ice distribution in a finite element global sea ice-ocean model. Ocean Model 27(3-4):114–129

Tolman HL (2009) User manual and system documentation of WAVEWATCH-III version 3.14. Tech Rep 276 NOAA-NWS-NCEP-MMAB

Van der Wegen M, Dastgheib A, Roelvink JA (2010) Morphodynamic modeling of tidal channel evolution in comparison to empirical PA relationship. Coastal Eng 57(9):827–837

Van der Westhuysen JA, van Dongeren AR, Groeneweg J, van Vledder GPh, Peters H, Gautier C, van Nieuwkoop JCC (2012) Improvements in spectral wave modeling in tidal inlet areas. J Geophys Res 117(C11)

WAMDI group (1988) The WAM model—a third generation ocean wave prediction model. J Phys Oceanogr 18:1775–1810

Wang ZB, Hoekstra P, Burchard H, Ridderinkhof H, De Swart HE, Stive MJF (2012) Morphodynamics of the Wadden Sea and its barrier island system. Ocean Coast Manage 68:39–57

Weisse R, von Storch H, Niemeyer HD, Knaack H (2012) Changing north sea storm surge climate: an increasing hazard? Ocean Coast Manage 68:58–68

Wu L, Chen C, Guo P, Shi M, Qi J, Ge J (2011) A FVCOM-based unstructured grid wave, current, sediment transport model, i. model description and validation. J Ocean Univ China 10(1):1–8

Yu Q, Wang Y, Flemming B, Gao S (2012) Modelling the equilibrium hypsometry of back-barrier tidal flats in the German Wadden Sea (southern North Sea). Cont Shelf Res 49:90–99

Zijlema M (2010) Computation of wind-wave spectra in coastal waters with SWAN on unstructured grids. Coastal Eng 57(3): 267–277